EVALUATING VIDEO AND BIOACOUSTICS SENSOR PERFORMANCE FOR A NOVEL HADAL WATER COLUMN PROFILER

A THESIS SUBMITTED FOR PARTIAL FULFILLMENT
OF THE REQUIREMENTS FOR THE DEGREE OF

BACHELOR OF SCIENCE

IN

GLOBAL ENVIRONMENTAL SCIENCE

MAY 2025

By
MATTIA DA FIENO

Thesis Advisor

DR. JEFFREY DRAZEN

I certify that I have read this thesis and that, in my opinion, it is satisfactory in scope and quality as a thesis for the degree of Bachelor of Science in Global Environmental Science.

THESIS ADVISOR

Dr. Jeffrey Drazen
Department of Oceanography

For my family first and foremost:

Dad, Mom, Loreno, Nik, Sadie, and Nonna among many others. The continuous love support I have received from all of you throughout my life is something that I would not have been able to complete this thesis or my undergraduate career without. I could not have asked for a better family to call my own.

Secondly, I would like to dedicate this to the amazing people I met and had the privilege of calling my friends throughout all four years of my undergraduate education and the amazing friends I have back home cheering me on. I will continue to carry a part of each and every single one of you as I go on in life.

Finally, I would like to dedicate this thesis to my friend Felix Kinkead who once said to me that "*the thing that separates you and me from everyone else is obsession*". Those words served as a very powerful source of motivation throughout the second half of my time in university and throughout the thesis process.

ACKNOWLEDGEMENTS

I would like to thank Dr. Jeff Drazen, Dr. Glenn Carter, and the rest of the hadal profiler team for the opportunity to work on this project for my G.E.S thesis and for Dr. Drazen's mentorship in my research. I would also like to thank Dr. Jessie Perelman for teaching me how to process and interpret the bioacoustics data from the Hadal Profiler. A special thank you to Agustin Da Fieno Delucchi for his help with the video detection algorithm. Additionally, a thanks to Devin Hogate, Tyra Arends, and the rest of the students on the HWCP Sea Trial cruises for their help at sea and on land throughout this process. Funding for this project comes from NSF-OTIC #2221749, the SOEST Dean's Office, the Ocean Exploration Trust (OET), and the WM KECK Foundation.

ABSTRACT

Due to its general inaccessibility, there are considerable gaps in knowledge about the bottom 6000-11,000 meters of the ocean, known as the hadal zone. Even within these extreme depths nearly all investigation has occurred on the seafloor so the water column above it remains almost unsampled. To address this inaccessibility, a new Hadal Water Column Profiler was designed to explore this zone. The goal of this project was to determine how well it performed, specifically, its video camera and bioacoustics sensors. A code-based annotation method was used to extract frames from the video in order to more efficiently identify organisms. The software ESP3 was used to create echograms of water column biomass. Both forms of data were compared with deployment factors such as rate of rotation and velocity on both ascent and descent to determine how these factors affected the quality of the data. As expected, the profilers travel speed had an influence of annotation quality, with an optimal rotation period of 5-10 seconds being determined for video observations and a slower velocity of 0.7-0.9 m/s also having an effect. While velocity does not seem to affect the bioacoustics data, a rotation period of 10 seconds is optimal. The second version of the automated frame detection algorithm substantially increased the number of detections, especially for harder to detect organisms such as fish and medusas. Further confirmation of sensor performance comes from the detection in both sensors of the location of the deep scattering layer in Hawai’i. Additionally, the profiler provided new acoustic profiles below 1000 meters.

Keywords: Hadal Water Column Profiler (HWCP), Deep-Scattering Layer (DSL), Bioacoustics, Camera transect, Rotation, Vertical Velocity, Backscatter, Diel Vertical Migration (DVM).

TABLE OF CONTENTS

LIST OF TABLES

LIST OF FIGURES

1.0 INTRODUCTION

1.1 The Hadal Zone and Hadal Ecology

The Hadal Zone is located between 6000-11,000 meters below sea level, accounting for 45% of the depth range of the ocean (Jamieson et al., 2010). It predominantly consists of 37 trenches which are formed in subduction zones created by the collision of tectonic plates (Gardner et al., 2014). As a result of this geological process, trenches run parallel to the nearest continental landmass; sloping downwards to a narrow, V-shaped cross section with the bottom only being 2-5 kilometers in width (Jamieson et al., 2010).

Temperature, pressure, and the availability of organic material are crucial in shaping the ecosystem and trenches have extreme physical conditions setting them apart from other marine environments. They have temperatures of 1.0-2.5°C below 6000 meters, with little temporal variation (Jamieson et al., 2010). The stability of these low temperatures are also influenced by cold deep-water currents, which are integral to global thermohaline circulation patterns (Vinogradov, 1962). In addition to consistent near-freezing temperatures, the hadal zone presents another challenge: immense pressure. Hydrostatic pressure increases at a rate of approximately 1 bar for every 10 meters of depth. At the bottom of the Mariana Trench at ~11,000 meters, the pressure is at 1100 bar making it approximately eleven hundred times greater than the atmospheric pressure at sea level or 16,000 psi (Jamieson et al., 2010).

One crucial factor in the ecology of the hadal zone is the limitation of food. While shallower environments rely on living photosynthetic organisms as the basis of their food web, the complete darkness of hadal trenches isolates them from surface-driven primary production. Instead, these ecosystems depend on the sinking export of organic particles (Sweetman and Witte, 2008). The predominant food sources for the hadal zone come from marine snow: the particulate matter consisting of various sources such as dead plankton, fecal matter from shallow water organisms, and other forms of detritus (Sweetman and Witte, 2008). It also needs to be considered that there are deep water currents that could horizontally transport nutrients for the organisms living in these trenches throughout the hadal zone (Vinogradov, 1962).

As a result of these conditions, organism biomass is not as abundant as the upper layers of the ocean. However, this does not mean that trenches are completely devoid of life. Organisms that inhabit these depths have evolved specialized adaptations, including highly stable enzymes, flexible cellular membranes, and pressure-resistant proteins, to maintain biological function under such extreme conditions (Jamieson, 2015). There is diversity in hadal trenches with fish, crustaceans, gastropods, and worms being some of the taxa found through sampling campaigns in trenches (Jamieson et al., 2010). Some organisms, such as various amphipods observed in various trenches are potentially endemic to the hadal zone (Lacey et al., 2016). These studies clearly demonstrate that life is capable of surviving in such extreme circumstances and that the hadal zone could be home to various species that are found nowhere else in the ocean.

1.2 Accessibility and Previous Research

To this day, many aspects of the hadal zone remain poorly understood. This lack of understanding is largely the result of extreme inaccessibility of these depths. Conventional research equipment cannot operate at hadal depths. Many early studies were conducted using dredges that relied on wires and winches (Beliaev, 1989). For instance, Vinogradov (1962) found the amount of plankton decreases quickly with increased depth in trenches. At hadal depths, the amount of wire spooled out would be nearly as heavy as the wires breaking strength, leading to lost gear and great challenges to sampling (Beliaev, 1989). Nevertheless, through considerable effort at dredge sampling, there is a baseline on what organisms live in specific depths on the seafloor in a number of trenches.

Over time, technological advancements have slightly improved the ability to study the hadal zone. While early research relied on dredges and trawls, modern explorations utilize devices such as remotely operated vehicles (ROVs) and free-falling landers equipped with cameras (Jamieson et al., 2010). However, there are still limitations. ROVs require support vessels that require an extensive amount of cables similar to a dredge or a net trawl. While landers are capable of reaching great depths without wires, they are designed to sit on the sea floor. Although they can collect temperature and conductivity data throughout the water column, the accuracy and quality of this data is affected by their design. While some CTD casts have been attempted in the hadal zone resulting in some data, the time and resources required are extremely costly as they rely on wire and equipment that is not necessarily rated for such extreme temperatures (van Haren et al., 2017). There are currently no devices that exist with the capacity to routinely and efficiently conduct water column studies past a depth of 6000 meters.

1.3 The Hadal Profiler

The newly developed Hadal Water Column Profiler (HWCP) is the first multidisciplinary instrument that can collect multiple samples a day and data from a trench water column (Figure 1). Unlike any scientific array attached to a wire, the HWCP travels through the water column autonomously, untethered to a ship. The HWCP has weights attached making it heavy enough to sink through the water column. A release mechanism is partnered with an altimeter so that when the profiler reaches a specified distance above the ocean floor, the release mechanism drops the weights causing the HWCP to become buoyant and return to the surface.

During any given deployment it collects data relevant to chemical, physical, and biological oceanography. The biological data is gathered through a standard definition video camera rated to 11 kilometers depth. Video data is gathered throughout the duration of each deployment alongside the bioacoustics. The camera is small so it can fit on the profiler, but the tradeoff is that it has standard (low) resolution compared to cameras commonly used on a Remotely Operated Vehicle (ROV). The video data serves as a method to identify what the bioacoustics sensor is potentially observing. The bioacoustics data is measured through a custom designed bioacoustics transducer sends out a ping of 200 kHz in a 10º cone. Unlike other bioacoustics collection typically gathered from a ship looking down at a water column (Perelman, et al. 2021), the Hadal Profiler will be travelling through the water column with its transducer pointed out horizontally. This should reduce the amount of surface and engine noise generated by a notable margin. The Geo-electromagnetic current meter (GMEC) requires the system to rotate which could result in a video with less objects passing by the camera or a less effective bioacoustics range, depending on the rotation rate.

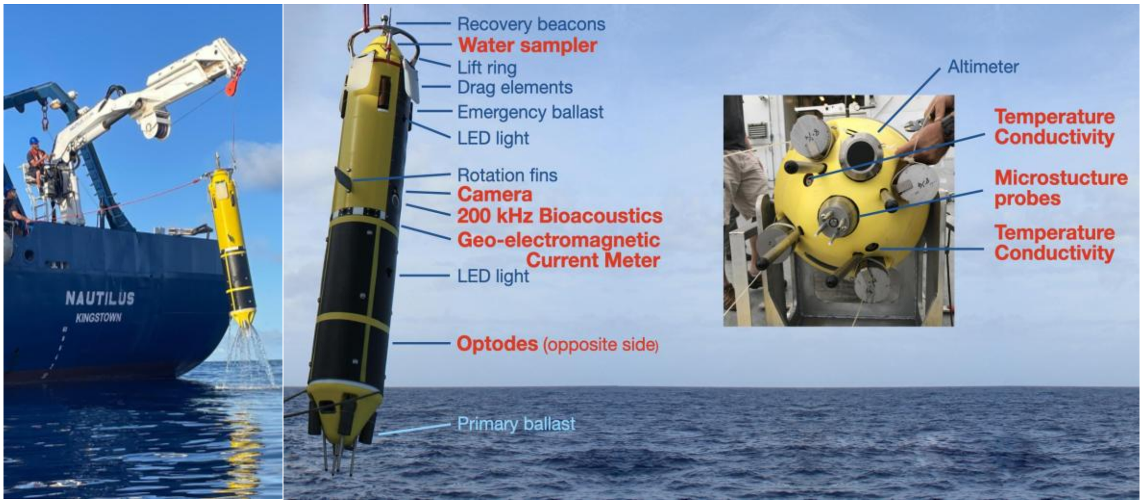

Figure 1: Left) the HWCP being recovered by the E/V Nautilus. Right) the sensor and key component layout of the HWCP.

1.4 Aim of Study

Since the profiler is in a constant state of motion throughout the data collection portion of its deployment, (surface time once completed is negligible) anything that passes by the camera will only be present for a short period of time. Additionally, with the rotation in effect anything passing by the camera will be moving at an angle across the field of view. For the bioacoustics, when a ping is emitted, it takes up to a second to reach an object in the water and relay the info back to the sensor. If the profiler is rotating while this is happening, a ping hitting something further might not make it back in time before the transducer is rotated too far to receive the signal. With this in mind, the question arises as to how these factors affect the quality and collection of data. The rotation and velocity can be altered to some extent with alterations to the lateral fins and primary and secondary ballast weights of the HWCP. Indeed, preset conditions could be determined so that a certain deployment could focus on different scientific goals favoring different sensors.

The aim of this study is to evaluate the performance of the HWCP video and bioacoustics sensors responsible for collecting biological data. Using data collected in Hawaiian water during test cruises I addressed two goals. First, compare the HWCP data to what we know of the vertical distribution and migration of pelagic fauna in Hawaiian waters. The deep scattering layer (DSL) is characterized by an increased density of organisms at a specific depth in the water column (Barham, 1963). In Hawai'i it is found between approximately 400-600 meters with variations based on the time of day (Drazen et al., 2023). These variations are a result of diel vertical migration (DVM): the active migration of a large quantity of organisms varying between day and night (Longhurst, 1976). The observation of this movement through the HWCP would prove particularly beneficial to better understanding the DVM patterns in the surface area of each deployment. Second, determine how rotation and vertical speeds of the HWCP affect the clarity of the video and bioacoustics and the range of animal detection in the bioacoustics. The rotation speed will likely affect the range of bioacoustics detection. The rotation can be altered to some extent with alterations to the lateral fins of the HWCP and vertical speeds can be altered by changing the ballasting of the system. Although these parameters need to be evaluated, I hypothesize that a slower rotation period and vertical speed will lead to a greater data yield from the video (better quality and easier to identify imagery) and bioacoustics sensors (larger range of detection).

2.0 METHODS

2.1 HWCP Deployments

While the HWCP is rated for 11km, this study was conducted using trial cruises in shallower waters in the main Hawaiian archipelago (Figure 2). Deployments were conducted on various research cruises on the R/V. Kilo Moana and the E/V. Nautilus with a total of 32 deployments occurring on 7 cruises. The cruises were located across various points in Hawai'i to test the profiler in different water depths and times of day (Table 1). Deployments conducted during both day and night enabled the evaluation of vertical migrations of organisms throughout the water column. While the deployment locations varied, they were selected based on logistical and weather-based constraints rather than being part of a structured study by design.

After deployment from the ship, the profiler descended through the water column to a set trial depth between 400 and 4000 meters or just above the seafloor. The rotation period and vertical velocity on a deployment were the result of modifications to the attached weights, lateral fins and drag elements of the HWCP. There were some changes as a result of currents, density, and other physical factors in the ocean. Throughout most deployments, the camera and bioacoustics sensor recorded data that was downloaded after recovery. At the target depth, the HWCP releases its weight and returns to the surface for recovery.

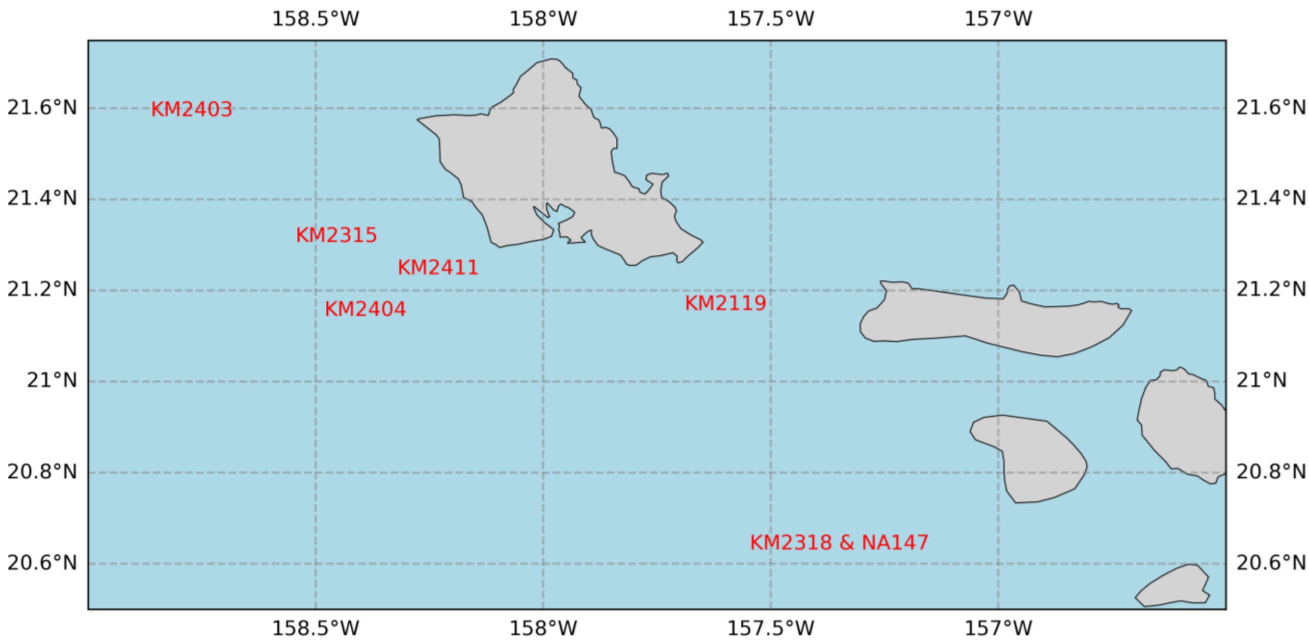

Figure 2: Map showcasing the approximate location of each of the HWCP Sea Trial cruises around the waters of O'ahu and Lana'i.

Table 1: HWCP free-falling deployments during testing cruises in the Hawaiian Islands. Each deployments date, time of deployment, location, and bottom and deployment depth is provided. Information on Rotation Period and Vertical Velocity on both ascent and descent for all HWCP deployments is also collected. Missing data is attributed to data that was not collected, HWCP problems stemming from the malfunction of different sensors, or data that was not analyzed for this study. Asterisks indicate deployments in which data was used for the study.

Deployment #	**Time & Date (UTC)**	**Day vs. Night**	**Position in Latitude and Longitude (°N, °W)**	**Deployment Depth (m)**	**Average Descent Rotation Period (s)**	**Average Ascent Rotation Period (s)**	**Average Descent Velocity (m/s)**	**Average Ascent Velocity (m/s)**	**Comments**
KM2119-05	03:27 9/12/2021	Night	21 14.696, 157 50.728	268	N/A	N/A	N/A	N/A	Data not analyzed for this deployment

KM2119-06	06:35 9/12/2021	Night	21 14.773, 157 50.969	279	N/A	N/A	N/A	N/A	Data not analyzed for this deployment
KM2119-07	17:42 9/12/2021	Day	21 2.409, 158 9.968	479	N/A	N/A	N/A	N/A	Data not analyzed for this deployment
KM2119-08	20:06 9/12/2021	Day	21 3.269, 158 10.380	1984	N/A	N/A	N/A	N/A	Data not analyzed for this deployment
*NA147-02	22:50 27/04/2023	Day	20 37.245, 157 9.093	1354	4.42	8.37	1.057	-0.77	

NA147-03	15:55 28/4/2023	Day	20 38.106, 157 11.140	1488	N/A	N/A	N/A	N/A	Deployment not dark enough for code
*NA147-04	00:10 29/04/2023	Day	20 38.148, 157 11.104	1473	5.41	5.48	0.891	-1.068	
*NA147-05	16:04 29/04/2023	Day	20 36.375, 157 13.691	2555	7.74	N/A	0.78	N/A	Profiler hits bottom
NA147-06	22:16 1/5/2023	Day	20 48.520, 157 3.337	377	N/A	N/A	N/A	N/A	Short deployment in light
*KM2315-01	03:33 24/09/2023	Night	21 8.248, 158 10.799	2158	6.68	4.44	0.783	-1.353	
*KM2315-02	17:55 24/09/2023	Day	21 17.797, 158 21.708	1979	5.4	6.17	0.778	-0.984	

*KM2315-03	00:29 25/09/2023	Day	21 17.832, 158 21.617	2570	4.27	9.16	0.928	-0.772	
*KM2315-04	03:54 25/09/2023	Night	21 17.798, 158 21.676	1979	154	53.16	0.928	-1.059	Code still worked, but potentially affected by light
*KM2315-05	17:25 25/09/2023	Day	21 17.801, 158 21.667	2786	5.16	5.92	0.781	-1.027	Profiler hits bottom
*KM2318-01	19:25 15/11/2023	Day	20 36.672, 157 9.197	1385	8.32	6.9	0.754	-0.895	
*KM2318-02	02:19 16/11/2023	Day	20 36.888, 157 9.673	1586	5.76	6.83	0.843	-0.892	acoustic data not good
*KM2318-03	20:09 16/11/2023	Day	20 36.736, 157 9.376	1515	248.67	73.23	0.937	-0.972	

*KM2318-04	23:49 16/11/2023	Day	20 36.925, 157 9.806	1535	231.62	109.77	0.853	-0.966	
*KM2318-05	03:19 17/11/2023	Night	20 36.757, 157 9.329	1414	44.65	28.1	0.856	-0.943	
*KM2403-01	01:10 17/04/2024	Day	21 34.392, 158 40.844	2507	18.05	42.1	0.784	-0.934	
KM2403-02	05:30 17/04/2024	Night	21 34.202, 158 41.958	2471	N/A	N/A	N/A	N/A	Deployment not dark enough for code
*KM2403-03	18:43 17/04/2024	Day	21 34.135, 158 42.396	2983	18.82	24.13	0.71	-0.938	
KM2403-04	22:56 17/04/2024	Day	21 30.892, 158 43.441	3986	N/A	N/A	N/A	N/A	No data outside of video

*KM2403-05	03:19 18/04/2024	Night	21 30.982, 158 43.330	4160	8.67	N/A	0.871	N/A	Profiler hits bottom (no azfp)
KM2403-06	21:52 18/04/2024	Day	21 17.912, 158 19.292	1980	N/A	N/A	N/A	N/A	Video not analyzed
KM2403-07	01:35 19/04/2024	Day	21 17.860, 158 19.086	1980	N/A	N/A	N/A	N/A	Video not analyzed
KM2404-01	01:19 21/04/2024	Day	21 13.463, 158 29.845	2675	N/A	N/A	N/A	N/A	Data not analyzed for this deployment
KM2404-02	23:01 21/04/2024	Day	21 19.513, 158 13.576	1092	N/A	N/A	N/A	N/A	Data not analyzed for this deployment

KM2404-03	2:03 22/04/2024	Day	21 19.519, 158 13.582	1092	N/A	N/A	N/A	N/A	Data not analyzed for this deployment
KM2411-01	3:58 23/07/2024	Night	21 19.224, 158 12.405	1030	N/A	N/A	N/A	N/A	Data not analyzed for this deployment
KM2411-02	16:14 23/07/2024	Day	21 15.626, 158 20.072	2501	N/A	N/A	N/A	N/A	Data not analyzed for this deployment

KM2411-03	00:05 24/07/2024	Day	21 22.569, 158 13.850	792	N/A	N/A	N/A	N/A	Data not analyzed for this deployment

2.2 Video Annotation

To help create a faster annotation process that can work reliably with a constantly moving camera, a video detection algorithm was developed. The program uses the black background of the HWCP video and extracts any frames in the footage that contain a predetermined set of colors. The colors were selected based on individual objects or organisms that pass by the camera during a deployment. This means that manual observations served as the foundation for this algorithm. To process colors into a format the algorithm could understand, a separate set of code was used to extract the hue, saturation, and value (HSV) of each color. HSV serves as a color model which was developed for computer graphics. The algorithm used the set HSV values given for each color, but has a threshold of 5,10,10 for hue, saturation, and value.

The video annotation algorithm went through two different versions that had a distinct set of colors (Table 2). A selection of 5 deployments (KM2135-01 & 02, NA147 02, 04, & 05) were chosen to be processed three times: once manually and the other two times using each version of the algorithm. This was to ensure that there was enough data to determine which method was the most effective. The first version of the algorithm only used 6 colors based on the organisms detected during manual annotations. Although this version was effective in identifying these colors, it did not always come to par with the manual annotation method (Figure 3). As a result, the second version with 10 colors was created to detect even more organisms that were not captured by version 1.

Table 2: The set of colors used in each version of the video detection algorithm with corresponding HSV values.

Code V1	Code V2	HSV Value
		13, 95, 121
		13, 68, 79
		18, 78, 82
		179, 104, 101
		177, 61, 118
		17, 52, 138
		17,74, 162
		3, 92, 142
		80, 230, 204
		5,146, 129

Once processed by the algorithm, the identified frames from the video are examined manually to identify individual organisms and other objects of interest. If an object was able to be identified into a broad taxon such as fish, medusa, or siphonophore, it would be considered a known individual. If the object were unidentifiable, it would be considered unknown. Additionally, if marine snow was identified, it would be omitted from the final classification as it is not in the area of interest. These video annotations for each individual animal or object were then related to the other HWCP sensor data (e.g. depth, temperature) using the time code of each frame.

2.3 Bioacoustics Sensor Processing

The Bioacoustics data was used to produce echograms of the water column in each deployment. The HWCP creates files that were converted into .01A files in order to be processed by ESP3. Additionally, each file was paired with an XML configuration file that allows the program to read them and includes calibration coefficients. Since ESP3 is designed to work with top-down shipboard bioacoustics data there were some modifications done to the exported data (Figure 3a). The data needs to be denoised using the acoustic sound leveling (ASL) filter in ESP3 to filter out unnecessary backscatter. The optimal denoising signal to noise ratio (SNR) is 3.0 resulting in considerably cleaner data presented as Area Backscatter Coefficient (ABC in m2/km2; Figure 3b). This denoising SNR was determined through testing multiple values from 1-5 to see which was most effective at filtering out unwanted backscatter. Then the data was binned into 10 second intervals and a range was set to select the desired data from the backscatter. Usually, a maximum range of 30 to 70 meters was sufficient depending on the furthest denoised values from the deployment. A minimum range of 2 meters was necessary since the first 2 meters from the profiler are too noisy to produce any readable data. The echograms produced were created by averaging the ABC values of each deployment split into day and night to properly separate the potential migratory differences as a result of DVM. Outliers were then removed from the echograms as they interfered with the display of the data, making it difficult to interpret. Outliers were determined to be any value that was at least one order of magnitude larger than a maximum value of 0.0014 S_a as these most likely represented larger objects near the surface or seafloor and were not indicative of the general biology in the area.

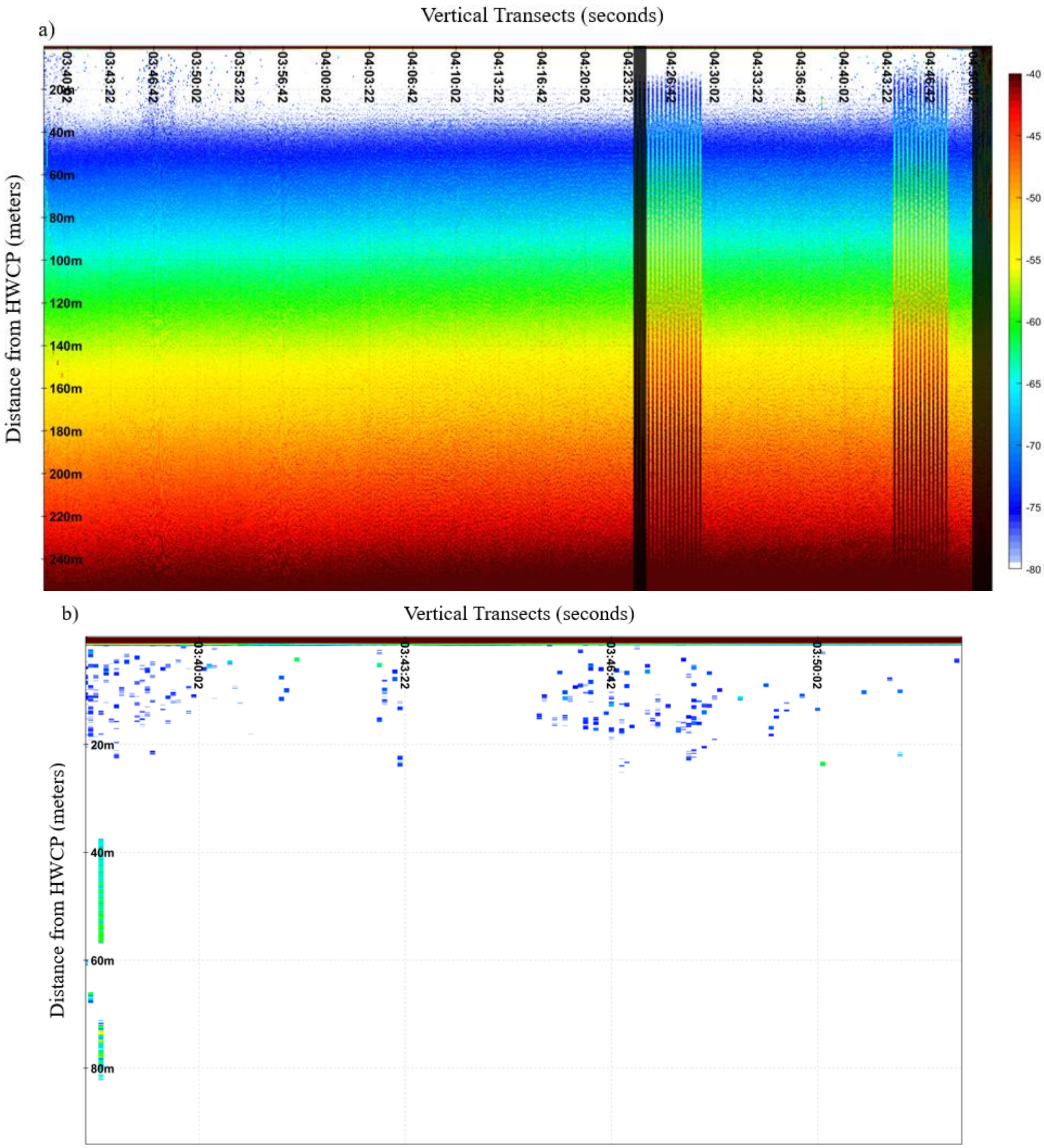

Figure 3: Echograms from an individual deployment (KM2315-01) in the a) raw format, and b) an enlarged portion of the filtered data. The black bars represent bad data that was removed.

3.0 RESULTS

3.1 Profiler Deployments

A total of 32 test deployments were conducted over 7 cruises between 2021 and 2024 (Table 1). Not every deployment produced usable data for video and bioacoustics analysis. For deployments NA147-03 and KM2403-02, there was an issue with the camera lighting that did not allow for proper video annotation. The lights made it so that the background of the video was too bright for the code to detect any of the set colors that could pass by the camera's field of view. Other deployments did not have any video to analyze due to the profiler not recording any video in its early trial stages. Other deployments were collected past the time of the present analysis (KM2404, and KM2411). The total number of deployments that ended up being used was 16 of the 32 total (Table 1). Each deployment varied in rotation period and vertical speed. Rotation speed ranged from a minimum period of 4.27 seconds to a maximum of 248.67 seconds (Table 1). The descent speed of nominally 0.75 m/s was based on microstructure measurements while the ascent while the ascent speed can be varied from about 0.8 m/s to 1.3 m/s based on scientific objectives for a particular cast.

3.2 Video Data

3.2.1 Automated frame event detection evaluation

The first version of the algorithm performed better than the manual annotation for fishes and crustaceans, but it did not catch certain organisms like medusa, that were observed with the manual method (Figure 4). After the addition of 4 more colors, the second version of the frame detection algorithm using 10 colors (Table 2) yielded the most results in almost every category (Figure 4). Importantly, the algorithm captured more animals than manual annotation. A deployment-by-deployment examination of the data also found that the second version of the algorithm identified all of the animals that were identified manually. In other words, it did not simply find different animals but found all animals identified manually plus additional ones that had been missed by a human annotator.

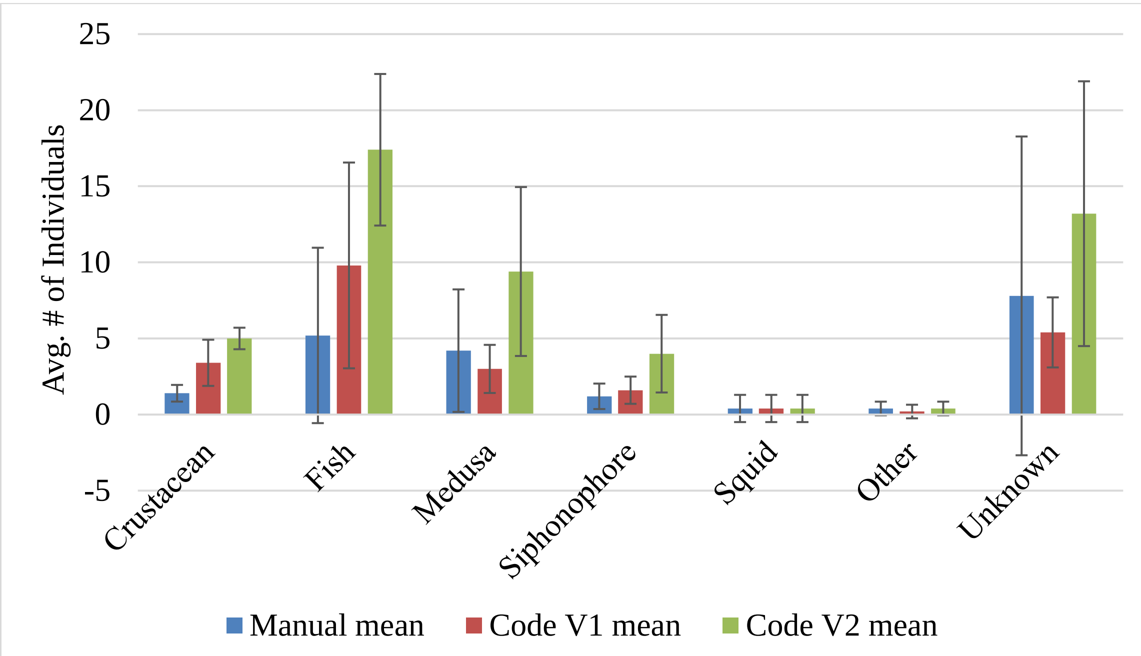

Figure 4: The comparison of three different methods to analyze the HWCP deployment footage averaged over 5 deployments. The manual method, the first version of the code with 6 colors, and the second version of the code with 10 colors (Table 2).

3.2.2 General video observations

The video captured a variety of organisms that passed by the camera. In total, there were 279 identified organisms across 16 deployments separated into 6 taxa (Fig. 5,6) and an extra category for identified objects that did not fit such as discarded larvacean houses or a jellyfish tentacle getting briefly stuck to the HWCP camera.

Identification was mainly based on the limited physical characteristics available and was mostly only capable of being done to the familiar taxonomic level. Color, orientation, movement, and shape were the predominant features used to help identify any organisms. The majority of identifiable or “known” organisms observed were medusa and fish that together made up approximately two thirds of the identifiable fauna (Figure 5). 120 observations were “unknowns”. Of the multiple organisms identified, the ones that were most clearly observed in the video feed were often squid, medusas, and siphonophores with fish being the most difficult to see clearly (Figure 6). Often times identification proved to be more difficult due to blurred imagery resulting in the many unidentifiable or unknown individuals that were detected.

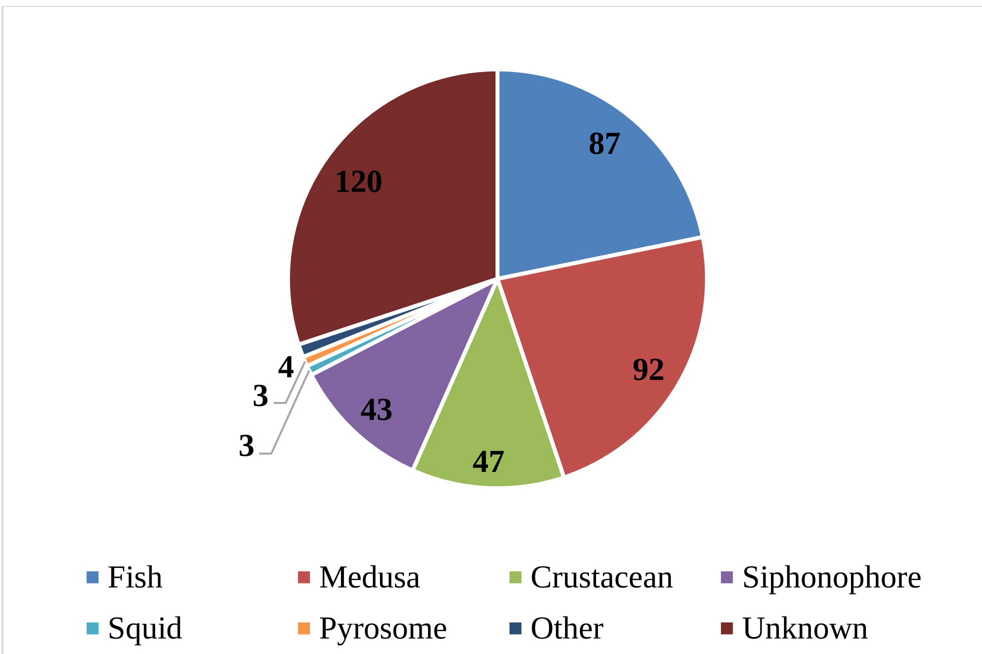

Figure 5: The total number of identified organisms split into 6 taxa, an “Unknown” category for organisms that were determined to be something other than detritus, but unidentifiable, and “Other”, a category for identified anomalies (see text for explanation).

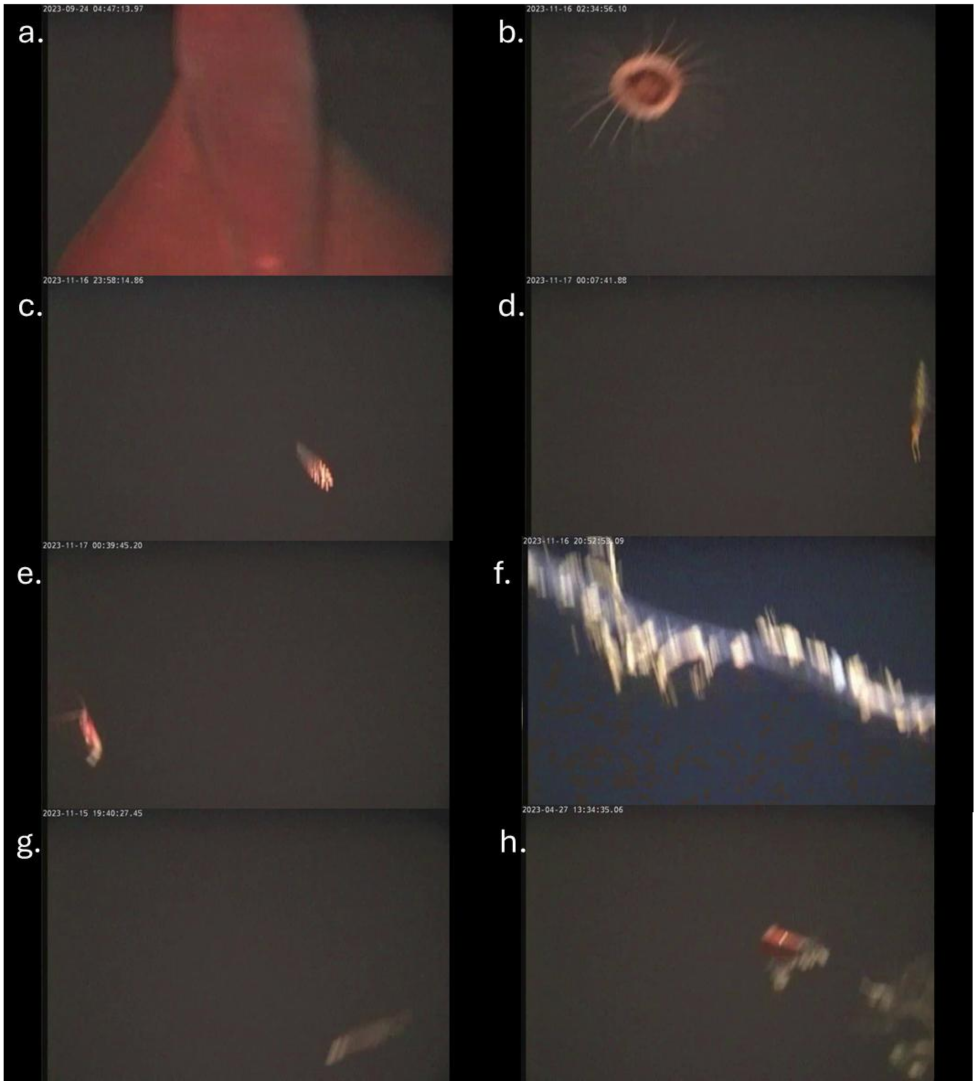

Figure 6: Images of organisms from various HWCP deployments all fitting into the classified taxa used in the annotation process. a) a larger squid that got close to the profiler. b) a red medusa. c) a Pyrosome. d) a cranchiid. e) a shrimp. f) a siphonophore close to the camera. g) a fish. h) something that fits into the category of “unknown”.

3.2.3 Vertical Distribution of Individuals

To acquire a complete distribution of organisms, all annotations were compiled and sorted by depth and taxa from the surface to 3000m (Figure 7). Three distributions were created based on the location of each deployment site. This depth was chosen as one that encompassed all but two of the deployments. Across all deployments, a larger number of individuals was detected between 500-800 meters. When factoring in both known and unknown individuals, the most are found at 600 meters, but the most diversity is between 700-800 meters. The only difference is that the offshore deployment data has a smaller concentration of biomass but still follows the observed trends.

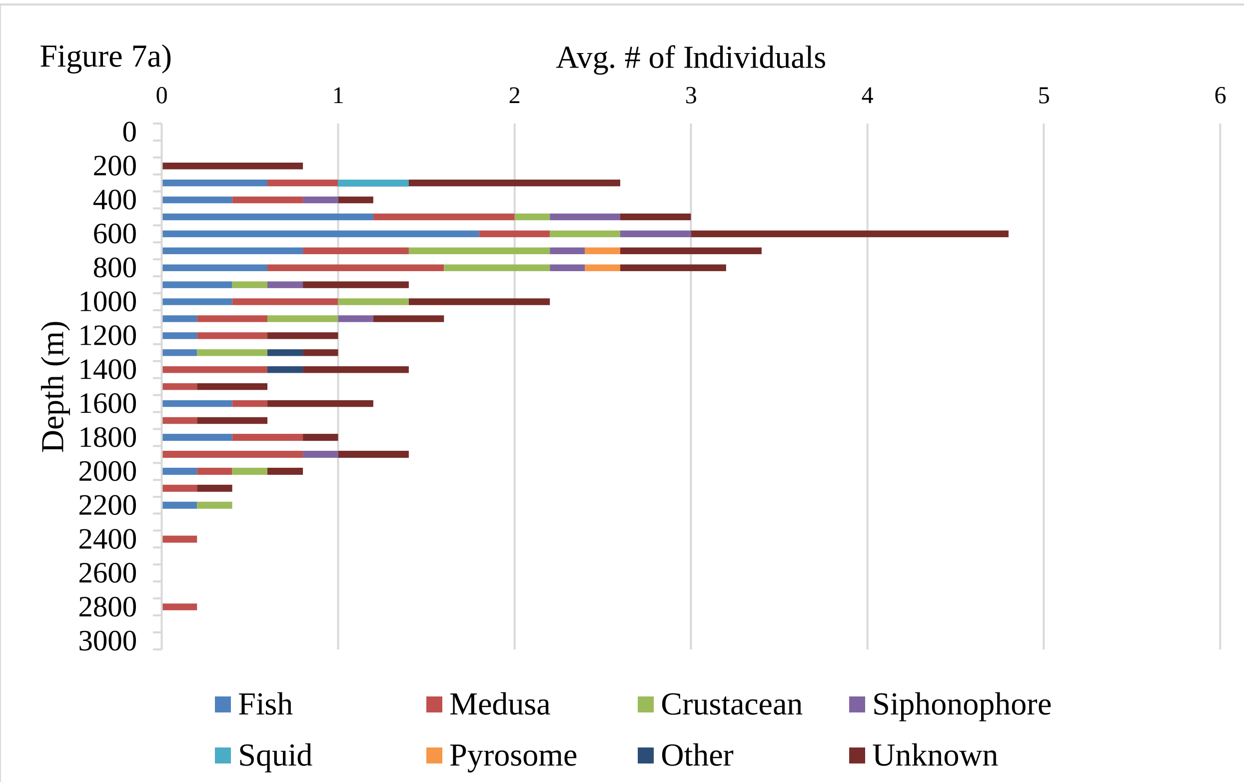

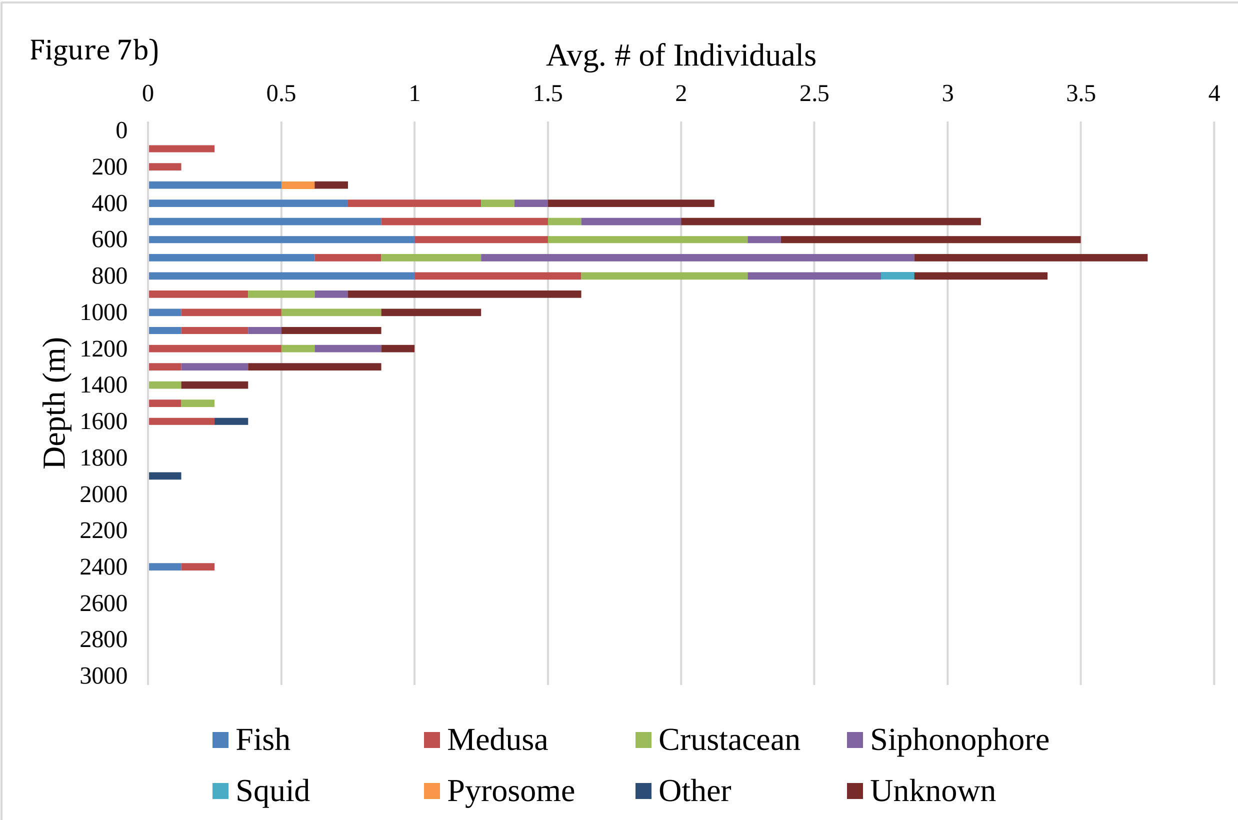
Figure 7b)
Avg. # of Individuals
0
0.5
1
1.5
2
2.5
3
3.5
4
Depth (m)
0
200
400
600
800
1000
1200
1400
1600
1800
2000
2200
2400
2600
2800
3000
Fish
Medusa
Crustacean
Siphonophore
Squid
Pyrosome
Other
Unknown

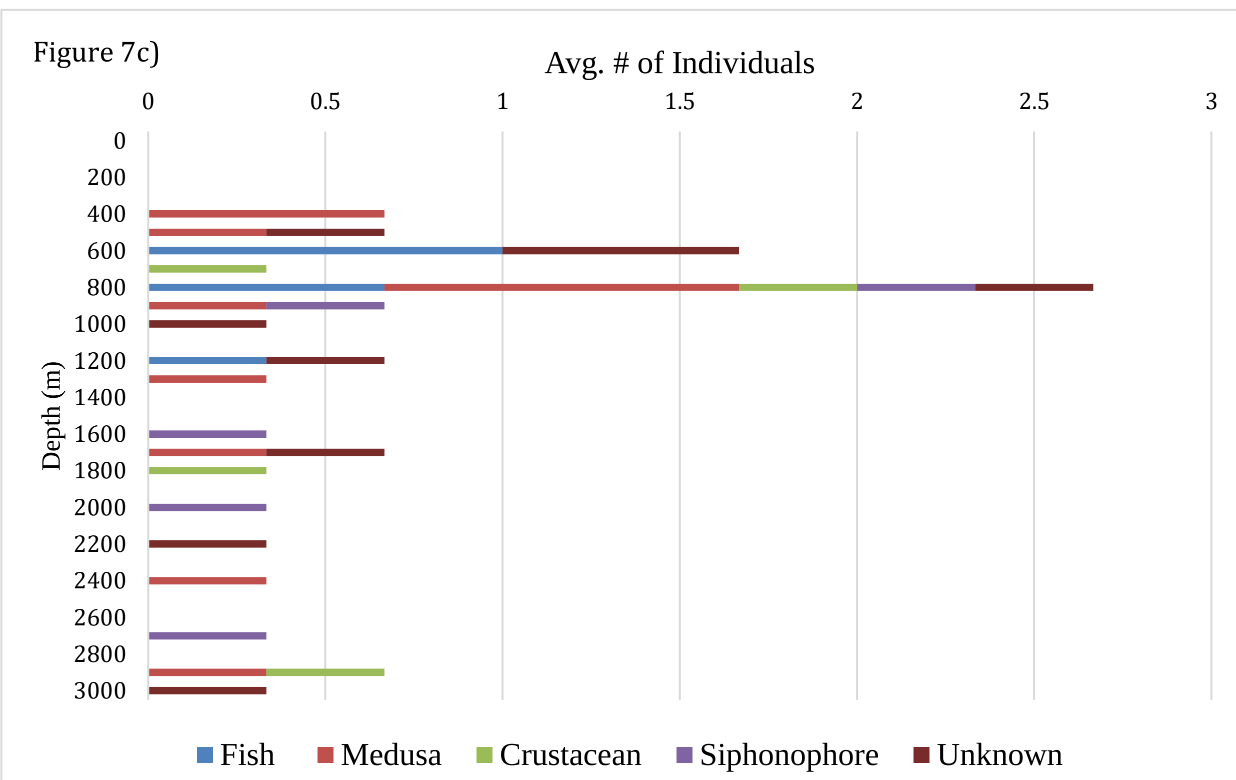
Figure 7c)
Avg. # of Individuals
0
0.5
1
1.5
2
2.5
3
Depth (m)
0
200
400
600
800
1000
1200
1400
1600
1800
2000
2200
2400
2600
2800
3000
Fish
Medusa
Crustacean
Siphonophore
Unknown

Figure 7: The average number of individuals found between 0-3000 meters categorized as a) KM2315 (n = 5), b) KM2318 & NA147 (n = 8) (both nearshore), and c) KM2403 (n=3) (offshore). Bins are 100 meters. Averages are taken over the number of deployments at each sampling site.

3.2.4 Vertical Velocity

Deployments that reached greater depth typically had greater numbers of animals observed due to integrating across more of the water column. In order to accurately compare the effect of vertical velocity or rotation on the video annotations, despite these varying depths of deployment, I analyzed the data to a depth to 1500m, a depth to which most of the deployments traveled to. To do so, any deployment shallower than 1500 meters was removed from the list leaving only 13 of the 16 remaining (NA147-02, KM2318-03, & KM2318-05 were excluded). The percentage of identified organisms was compared to those marked as "unknown". Each deployment was then split into ascent and descent due to the general increase in speed on ascents compared to descents. The deployments with the highest percentage of known individuals observed across 1500m all appeared within 0.7 and 0.9 m/s (Figure 8), though there was no strong relationship evident. Additionally, almost every deployment descent was slower than its ascent (Table 1, Figure 8).

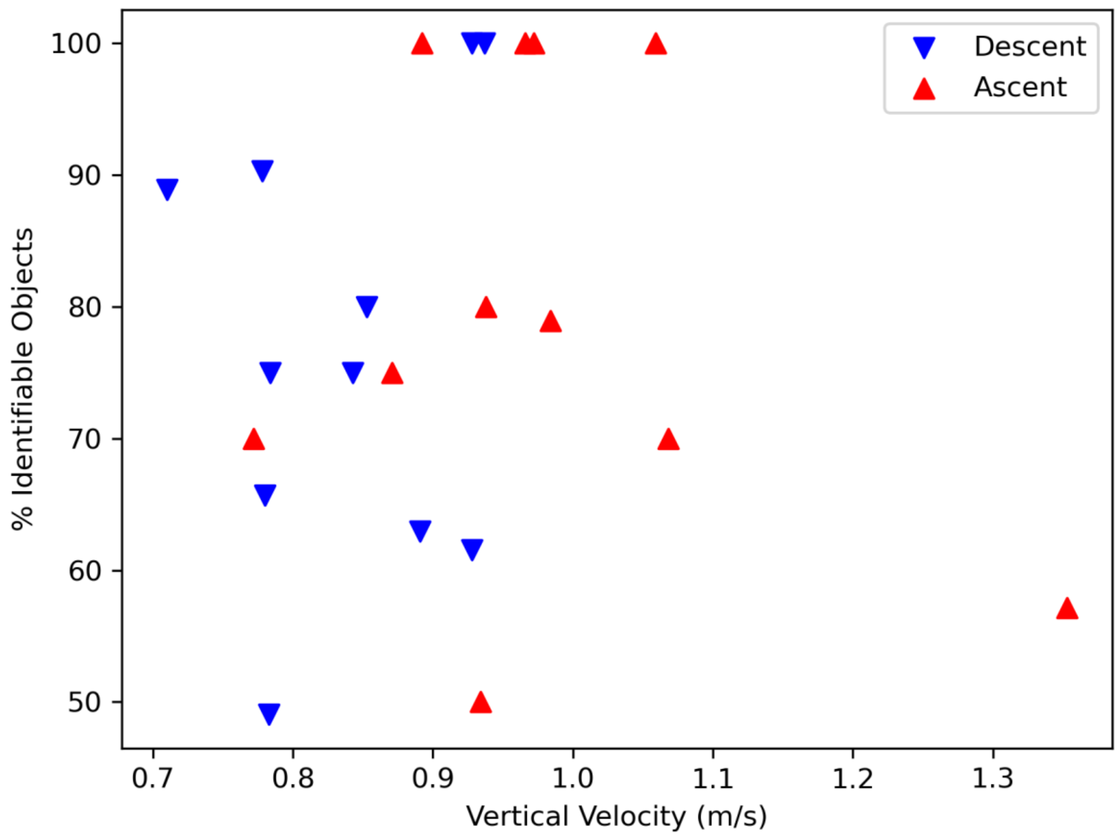

Figure 8: The percentage of identified individuals during a deployment depending on the vertical velocity of the HWCP. Descent is marked in blue while ascent is marked in red.

3.2.5 Rotation Period

Similar to the vertical velocity analysis, the same cutoff of >1500 meters was used resulting in the same 14 deployments being used with the same split of ascent and descent. In this case, a large majority of the deployments have fast rotation periods between 5 and 10 with various percentages of identifiable organisms. However, the deployments with 100% identifiable organisms are distributed amongst various rotation periods (Figure 9a). When comparing the number of identifiable organisms, the highest percentage of identifications happened between 5-10 seconds (Figure 9c). When looking at just deployments with rotation between 5 and 10 seconds, there is no apparent relationship to percentage of known individuals (Figure 9b).

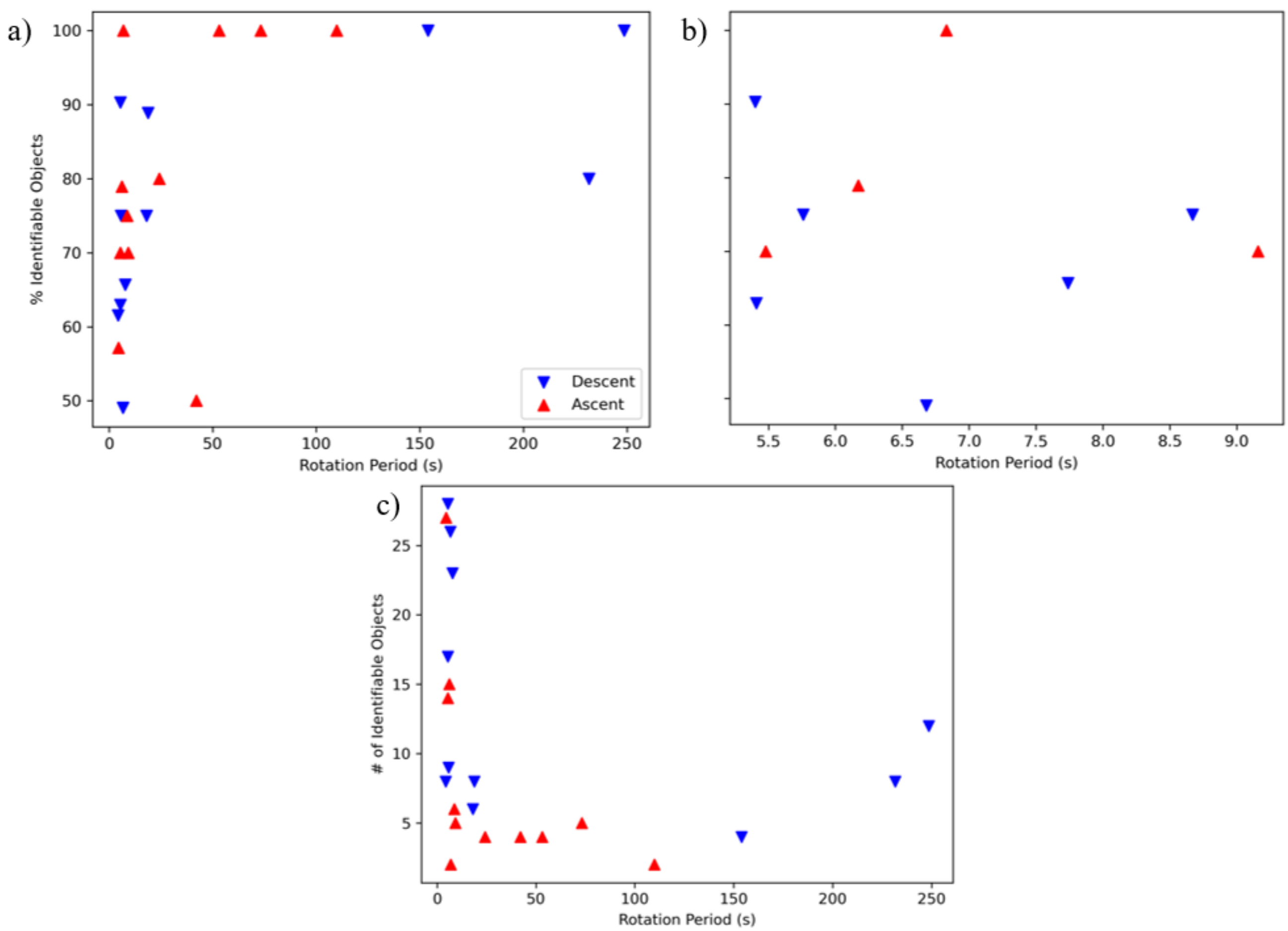

Figure 9: a) the percentage of individuals identified during a deployment depending on the rotation period of the HWCP and focused between b) 5 and 10 seconds. c) demonstrates the number of organisms detected in a deployment depending on the HWCP rotation. Descent is marked in blue while ascent is marked in red.

3.3 Bioacoustics Data

3.3.1 Rotation period

To assess the effect of the HWCP's rotation period, it was compared to the maximum detected distance of a deployment on both the ascent and descent. The same parameters were used for the maximum distance as the number of known objects from video with the same cutoff depth of >1500m. Similarly to the video, the majority of maximum distances were reached when the profiler was rotating at an interval between a 4- and 20-second rotation period (Figure 10a). The furthest distance from the profiler was 90 meters and maximum distance increases with rotation period in this section (Figure 10b). The upper quartile of the data shows that 75% of the detection distances throughout every deployment occur within 25m of the profiler in that 4-20 second range (Fig. 10c).

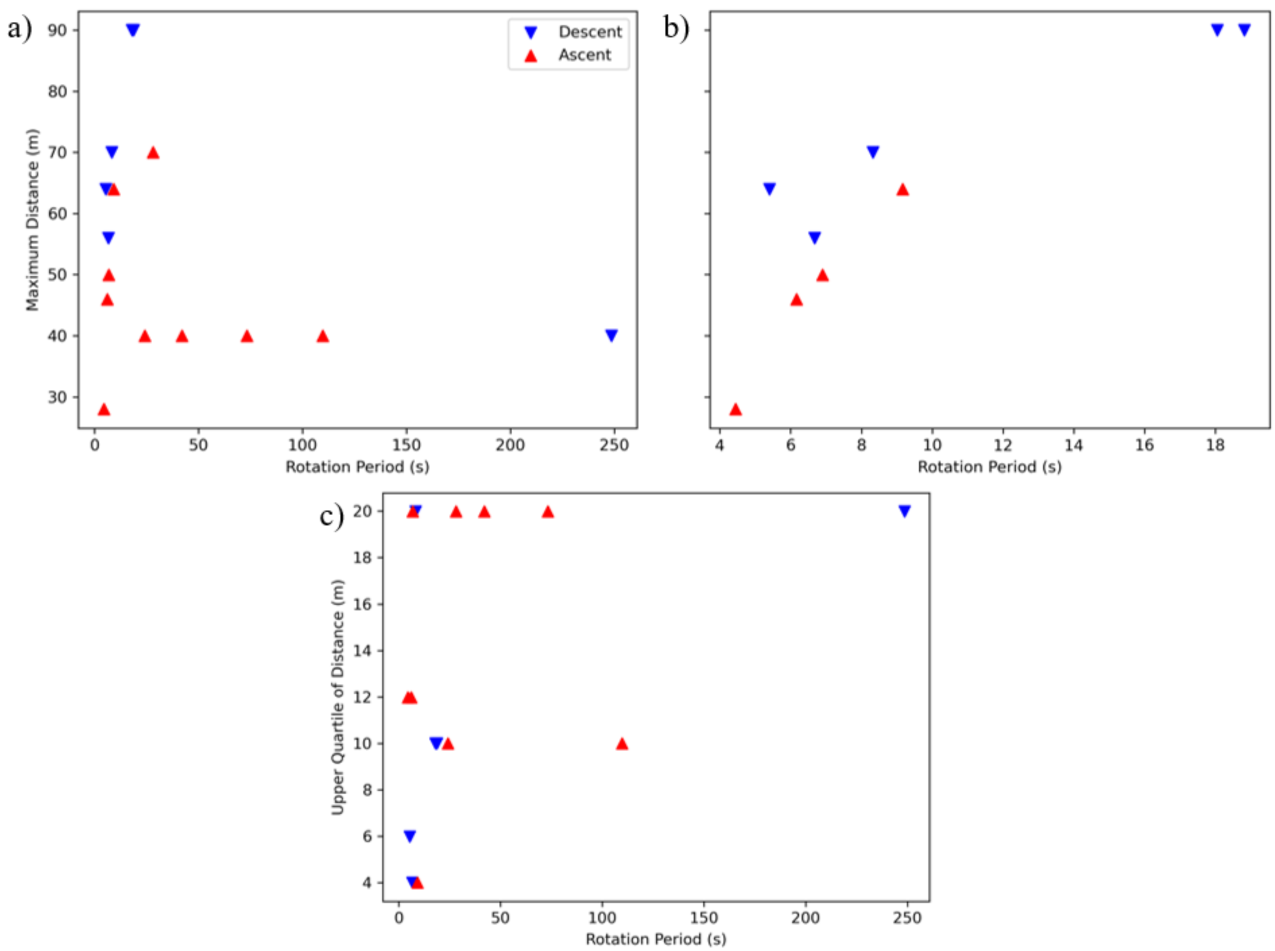

Figure 10: a) the maximum distance detected by the acoustic transducer in comparison to the HWCP's rotation period for various cruises and a focused view b) between 4-20 seconds. c) The upper quartile of the same data. Deployments are separated by ascent and descent.

3.3.2 Vertical velocity

For vertical velocity the majority of the deployments were below 1 meter per second with some variation in the maximum distance of acoustic targets (Figure 11). The shortest detection distance corresponds to the highest vertical speed of over 1.3 meters per second (Figure 11). As velocity decreases, the maximum distance the HWCP can reach increases to a maximum of 90 meters.

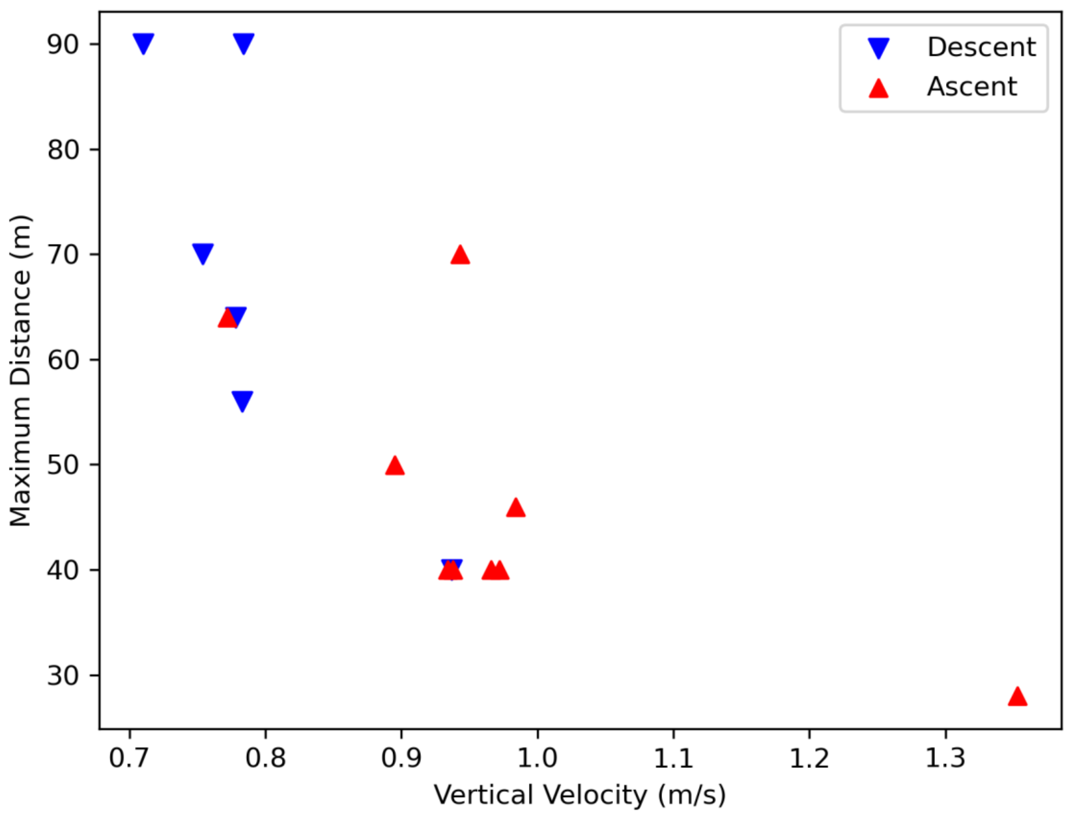

Figure 11: The maximum distance detected by the acoustic transponder in comparison to the HWCP’s vertical velocity for various cruises separated by ascent and descent.

3.3.3 Echograms

The first OTIC funded cruise (KM2315) was the only one to produce echograms with averages of both day and night taken (Table 1) with all deployments being conducted off west O'ahu (Figure 1). Each individual deployment corresponding to time of day was binned and then the average of each deployment was taken at each depth. Both day and night echograms show an increased concentration of biomass at both the surface (0-200m) and deeper at approximately 500m (Figures 12 & 13). There are also much smaller peaks at approximately 2000m during the day (Figure 12). In contrast, at night, the 500m peaks are much smaller than during the day, there are no small 2000m peaks and instead there is a peak around 1000m on the descent and at least on the ascent peak values are higher near the surface at night (Figure 13).

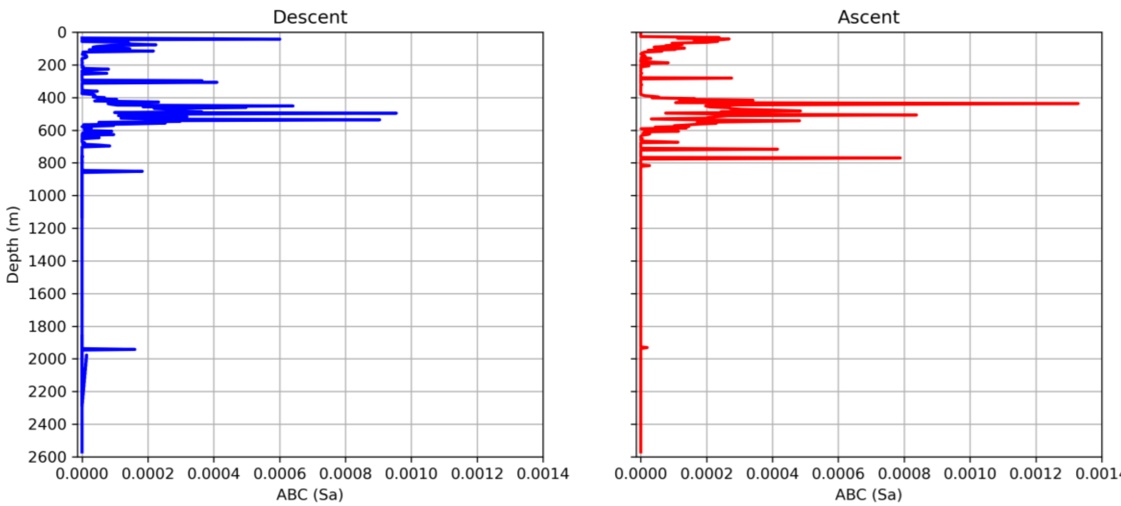

Figure 12: Echograms for the descent and ascent of KM2315. The average number is taken over all deployments (n =2) that took place during the day.

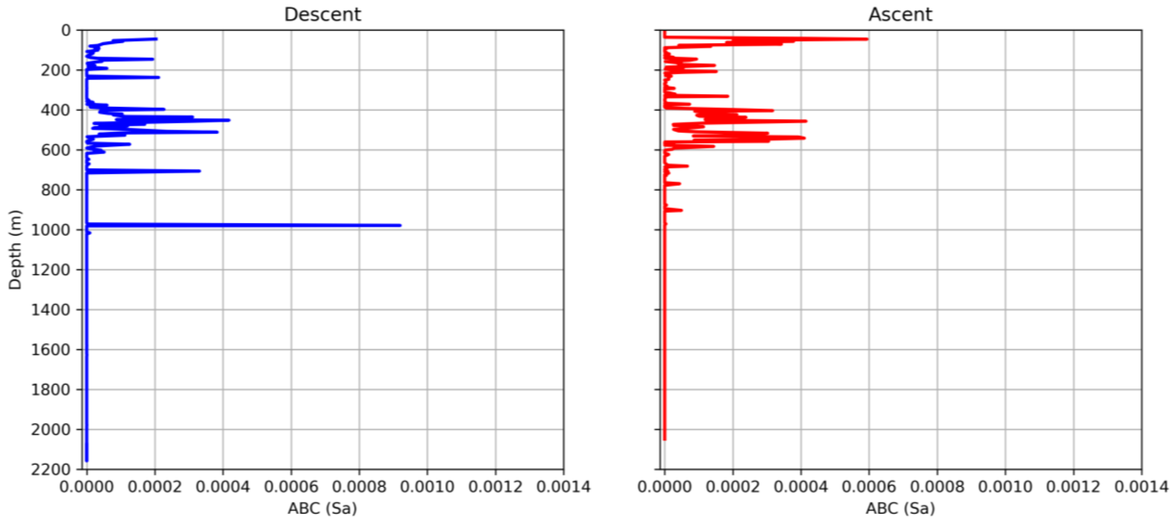

Figure 13: Echograms for the descent and ascent of KM2315. Averaged over all deployments (n=2) that took place at night.

During KM2318, which was off the coast of Lana'i (Figure 1), the distribution of biomass was considerably more widespread. There were still some peaks around the surface and 500m, but they were less defined than in KM2315 (Figure 14). There were also smaller peaks located below 1000m with the deepest being below 1400m (Figure 14). In comparison to the day average of KM2315 (Fig. 11), the S_a values were much smaller.

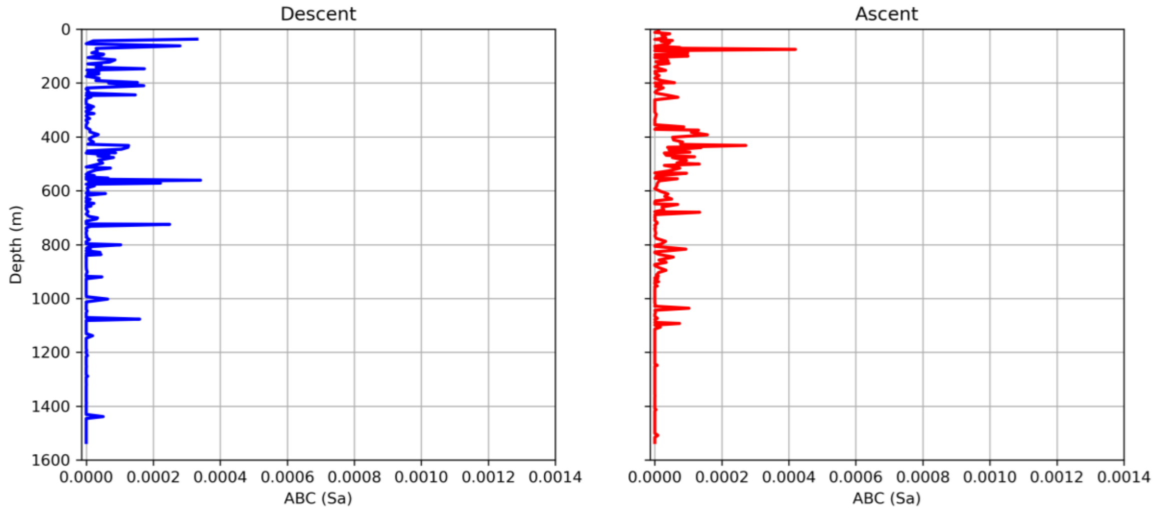

Figure 14: Echograms for the descent and ascent of KM2318. Averaged across all deployments (n =3) that took place during the day.

During KM2403, which took place off the west coast of O'ahu further north and offshore from the deployments done on KM2315 (Table 1), the distribution appears more similar to that of the day average of KM2315 with peaks at both the surface and at 500m with additional peaks present between 1300 and 1800 meters (Figure 15). The S_a values were also generally smaller than what was observed on KM2315 (Fig. 15).

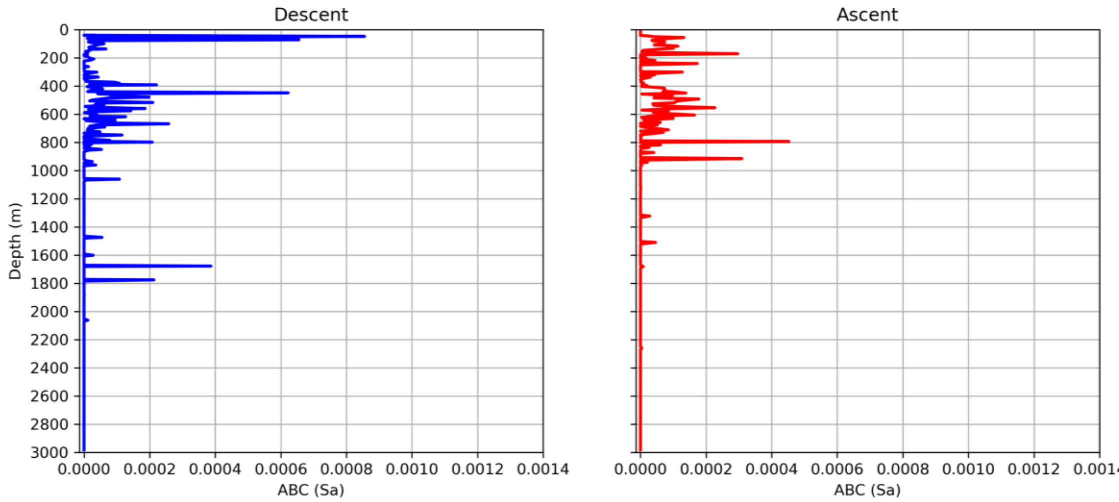

Figure 15: Echograms for the descent and ascent of KM2403. Averaged across all deployments (n=3) that took place during the day.

3.3.4 Comparison to video

Using an individual deployment, a comparison can be made to see whether or not the video and bioacoustics identify similar vertical profiles of their measurements. Deployment 2315-02 was used for its large number of annotations. The top peak in ABC at 100m does not correspond to observations in video. However, the main ABC peak from 400-600m does correspond to many observations in video. The same is true at ~2000 meters (Figures 16a & 16b). The most intense ABC peak at 500 meters consisting of 4 fish, 2 medusas, and a crustacean in the video observations (Figure 16b).

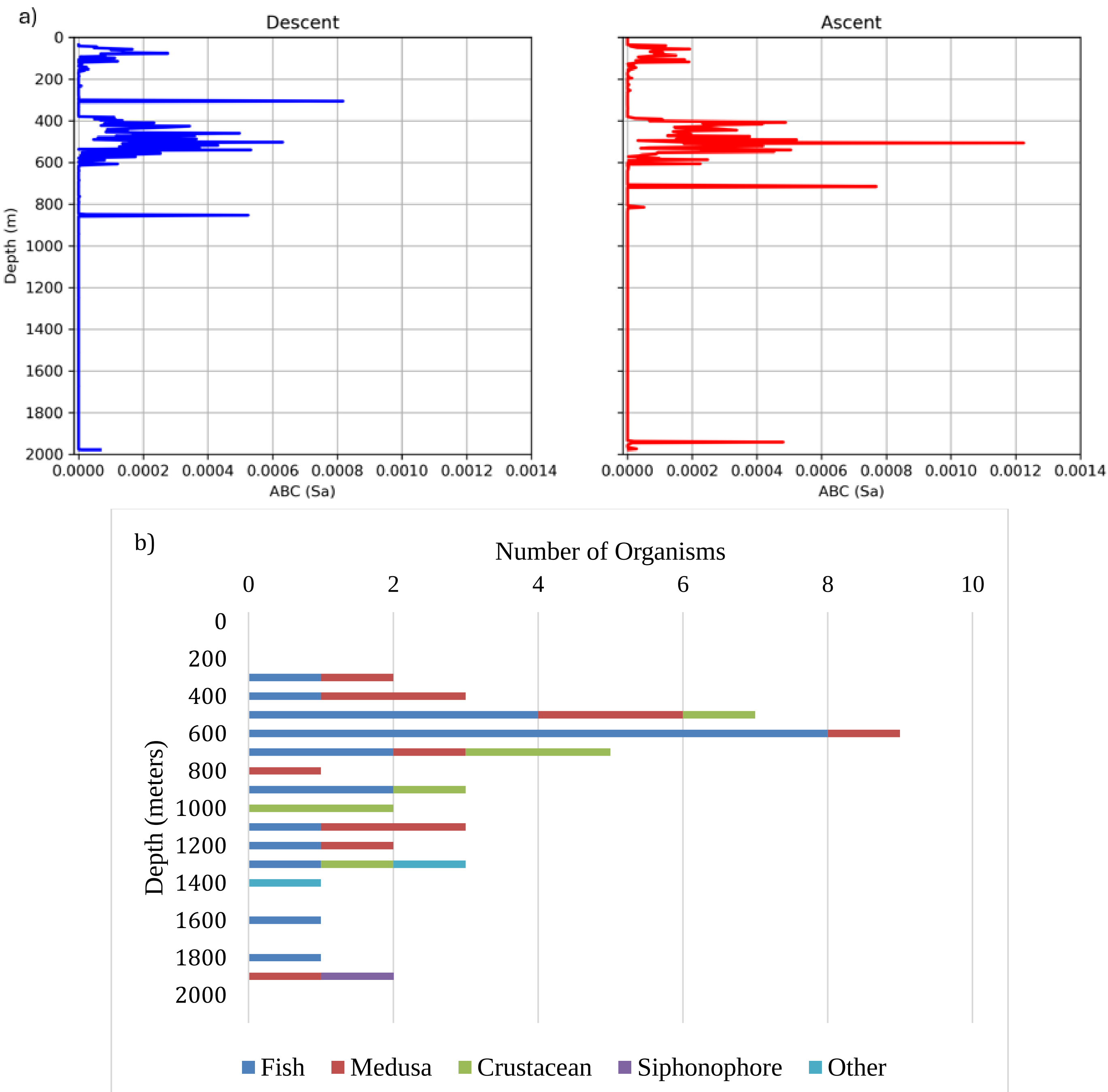

Figure 16: Plots showing a) individual echograms of KM2315-02's ascent and descent and the b) distribution of identified individuals across depth classified by taxa for the same deployment.

4.0 DISCUSSION

These trials provided the first detailed analysis of how the HWCP deployment parameters affect both video and bioacoustics data collection. The data yielded an important set of results that will help optimize future profiler deployments that will reach up to 11km in depth. Furthermore, the trials offered a comparison between video and bioacoustics observations while creating vertical acoustic profiles that extend past 1000m.

4.1 Effect of deployment parameters

The data from the trial cruises shows that the rotation period did not have a large effect on the quality of the results obtained from the video data. The deployments where 100% of the organisms were identifiable also varied across a very slow and very fast rotation period meaning that there is likely no correlation between quality of video data and the rotation period. The initial hypothesis that a slower rotation period would lead to more video observations was not correct. Instead, there was an optimal range of a 5-10 second rotation period that led to more organisms being seen in the video (Figure 9c). A faster rotation period means that more of the water column is being visualized leading to more organisms passing by the camera. One point of consideration is that the algorithm may help detect organisms at a higher rotation period since it relies on color and not something that is dependent on the rotation such as movement.

In regard to the bioacoustics, our hypothesis that fast rotation periods could limit detection distances was supported. For rotation periods between 4 to 20 seconds there was an increase in the maximum distance at which the transducer recorded objects as rotation period increased/rotation speed slowed down (Figure 10b). Additionally, 75% of the maximum distances the transducer was able to detect were within 25 meters of the HWCP. This suggests that regardless of the parameters, the bioacoustics data will still be affected by the profiler's movement. The other consideration is that the average acoustic profiles produced from the HWCP data produced data similar to expectations from shipboard systems with biomass peaking from 400-600m (Drazen et al., 2023). Therefore, I conclude that a rotation period of 10 seconds is a good parameter that allows for both good video and bioacoustics data. This recommended rotation period matches the 10 second rotation period that the GMEC for it to collect solid current data (Sanford et al., 1978).

Vertical velocity does seem to have an influence on the data produced; it has a much smaller effect than the rotation period. The highest number of individuals found in deployments occurred with vertical speeds of 0.7-0.9 meters per second (Figure 8). This suggests that slower speeds through the water column yield better results with more identified individuals as I had hypothesized. A slower velocity resulted in a larger detection distance for the bioacoustics with a maximum detected distance of 90 meters found in this 0.7-0.9-meter range. Additionally, the fastest recorded velocity of over 1.3 meters per second resulted in the shortest maximum distance (Figure 11).

Given a weaker influence of vertical velocity, at least within the range evaluated (0.7-1.3 m/s), the parameter that should be minded the most is the rotation period. Fortunately, it is somewhat customizable as the lateral fins can have their resting angle or size altered in order to change the rotation period. Weight of the ballast can also be set to reduce the speed at which the HWCP descends through the water. The most important thing to consider is that the bioacoustics data is going to be affected more than the video data which could partially be the result of the frame detection algorithm being able to extract frames regardless of the speed at which something passes by the camera.

4.2 Effectiveness of frame detection algorithm

The second and most current version of the frame detection algorithm proved to be the most effective in detecting animals or objects of interest in the HWCP deployment videos. The use of ten colors instead of six (Table 2) considerably expanded the number of detections, often finding those organisms such as fish or medusas that were not bright red and harder to see when passing by the camera. In the case of fish, the second version of the algorithm almost doubled the average number of fish detected (Figure 4). One consideration with this algorithm is that it was created very specifically with the HWCP videos in mind. Specifically, the algorithm was designed for video with a dark background with a lower resolution being contrasted with a blurry object that is a specific color (Figure 6). Other detection algorithms that can also classify species such as the one used in Salaman et al., (2020), require a large training dataset that accounts for factors such as species, background movement, light levels, and other oceanic conditions. Jalal et al., (2020) also states that there is no existing simple solution to automatically detect organisms from video and opts for a hybrid approach between automated and manual frame analysis to make work easier. Thus, the approach taken for the HWCP video is an effective start to identify organisms that pass by the camera as it allows for quicker detection of organisms but leaves the identification to humans.

4.3 Comparison of video and bioacoustics

One of the main goals of this study was to see if the video data and bioacoustics data were comparable, at least in a relative sense. Unfortunately, the first 2 meters of bioacoustics data are noisy and unusable and have to be filtered out, which is common for these types of systems (Ryan et al., 2015). Though distance is not measured by the video, anecdotally, most animals observed were smaller in size and most likely within those first 2 meters away from the HWCP. Some larger animals like siphonophores were observed, probably at greater distances, but they were much rarer. Nevertheless, the depth profile of video annotations can provide some context as to what organisms the transducer was scanning. Buscaino et al., (2023) ran a shallow water study using both video and bioacoustics data to identify different fish species and found that while video proved more effective in identification, the two systems yielded "complementary results" that can be combined. Within individual deployments there are matching peaks of biomass distribution (Figure 16) and comparing the two could potentially provide some validation if it is assumed the community near to the camera is representative of that a bit farther away. For example, in the case of 2315-02 where both the video and bioacoustics have large peaks at around 500 meters, the video annotation says that the distribution is predominantly made up of fish (Figure 16a). With the majority of the acoustics data being recorded within 25 meters (Figure 10c), there is a higher chance that the organisms the camera detects are representative of the ones at a greater distance. One part of the water column that the bioacoustics covers better than the video is the near surface zone to about 200m. Since the detection algorithm works best in complete darkness, sunlit areas will be harder for it to detect animals. Fortunately, this system was designed to sample much deeper parts of the water column. Based on the results provided by the HWCP and the recommendation from Buscaino et al., (2023), the camera data will prove useful to interpret and further understand the bioacoustics data.

4.4 Water column models and organism distributions

Through both the video and bioacoustics data, the largest peaks of occurrence and ABC were between 400 and 600 meters (Figures 10,12,14,15, &16). This corresponds well with the findings of Drazen et al. (2023) that found a similar peak backscatter from ship-based observations off Hawai'i island and its assessment of where the DSL is found in Hawaiian waters. The difference in ABC intensity between the echograms taken during the day and night also indicates that the biomass that was initially there moved shallower throughout the night (Figs. 12 & 13) as expected from DVM (Parra et al., 2019). On average across all deployments, every single identified taxon was found within this layer with the majority being fish, medusas, and crustaceans (Figure 9b). One advantage this data has is that it goes past what can be seen by top-down acoustic sounders from ships that often have a depth limit of 1000m (Barham, 1963), depending on frequency. This provides the opportunity for new insights as to where biomass is distributed below the deep scattering layer and even further past 1000 meters.

4.4.1 Bioacoustics profiles past 1000m

Although ABC values below 1000 meters were low, there is not a complete absence of life. Across the various acoustic profiles, there are multiple peaks below 1000m with the deepest peak being found slightly above 2000 meters (Figures 13,14,15, &16). The greatest number of peaks below 1000 meters were found further offshore of the west O’ahu coast with a larger set of peaks around 1400-1600 meters (Figure 15). These peaks are much smaller than their shallower counterparts with most of them being half the size if not smaller. The video data also found organisms below 1000 meters. As it gets deeper, fish begin to decrease as the predominant taxon with medusas and crustaceans, and siphonophores becoming the more dominant group (Figure 9b). These taxa may comprise sporadic or episodic depth layers of higher biomass, previously undetected by shipboard systems. This is also an illustration of the potential importance of the HWCP when it is finally deployed to hadal depths, which have yet to be explored.

5.0 CONCLUSION

The HWCP biological sensors proved to be an effective method of capturing both video and bioacoustics data. The results indicate that an optimal deployment configuration is a rotation period of 10 seconds and vertical velocities of just under 1 m/s. These parameters allow for the profiler to capture a greater range of organisms throughout the water column. The bioacoustics data provided comparable depth profiles of ABC to those from the upper 1000m from shipboard systems in the region (Domokos, R. 2022) and added new insights into the distribution of biomass below 1000 meters. The complementary video data, while not exactly comparable to the bioacoustics, provided potential answers to what organisms are located at those depths where backscatter was high. The second version of the frame detection algorithm further improved on organism detection in comparison to a manual annotation process, but it is an algorithm specific to the current HWCP video system. The Hadal Water Column Profiler has the potential to revolutionize hadal research by allowing for sampling of the water column that has not been done before at hadal depths. Future deployments of the novel HWCP into trenches will improve the understanding of how one of the least understood regions of the planet truly functions.

LITERATURE CITED

Barham, E. G. (1963). Siphonophores and the Deep Scattering Layer. *Science.*, *140*(3568), 826–828. https://doi.org/10.1126/science.140.3568.826

Beliaev, G. M., (1989). Deep Sea Ocean Trenches and their Fauna.

Benoit-Bird, K. J., & Au, W. W. (2004). Diel migration dynamics of an island-associated sound-scattering layer. *Deep-Sea Research.*, *51*(5), 707–719. https://doi.org/10.1016/j.dsr.2004.01.004

Buscaino, G., Papale, E., Gabetti, A., Busetti, C., & Ceraulo, M. (2023). Fish biodiversity assessing using bioacoustics and video data from a marine shallow water observatory. https://doi.org/10.61782/fa.2023.1085

Drazen, J. C., Clark, B. H., Gove, J. M., Phipps, J. E., Copeland, A. M., Lecky, J., Green, J. A. M., Kobayashi, D. R., Turner, J. R., Whitney, J. L., & Williams, G. J. (2023). Near-island enhancement in mesopelagic micronekton assemblages off Hawaiʻi. *Deep-Sea Research. Part I, Oceanographic Research Papers*, *199*, 104107-. https://doi.org/10.1016/j.dsr.2023.104107

Domokos, R. (2022). Seamount effects on micronekton at a subtropical central Pacific seamount. *Deep-Sea Research. Part I, Oceanographic Research Papers*, *186*, 103829-. https://doi.org/10.1016/j.dsr.2022.103829

Gardner, J. V., Armstrong, A. A., Calder, B. R., & Beaudoin, J. (2014). So, How Deep Is the Mariana Trench? Marine Geodesy, 37(1), 1–13. https://doi.org/10.1080/01490419.2013.837849

Ichino, M. C., Clark, M. R., Drazen, J. C., Jamieson, A., Jones, D. O. B., Martin, A. P., Rowden, A. A., Shank, T. M., Yancey, P. H., & Ruhl, H. A. (2015). The distribution of benthic biomass in hadal trenches: A modelling approach to investigate the effect of vertical and lateral organic matter transport to the seafloor. Deep-Sea Research. Part I, Oceanographic Research Papers, 100, 21–33. https://doi.org/10.1016/j.dsr.2015.01.010

Jalal, A., Salman, A., Mian, A., Shortis, M., & Shafait, F. (2020). Fish detection and species classification in underwater environments using deep learning with temporal information. Ecological Informatics, 57, 101088-. https://doi.org/10.1016/j.ecoinf.2020.101088

Jamieson, A. J., Fujii, T., Mayor, D. J., Solan, M., & Priede, I. G. (2010). Hadal trenches: the ecology of the deepest places on Earth. *Trends in Ecology & Evolution (Amsterdam)*, *25*(3), 190–197. https://doi.org/10.1016/j.tree.2009.09.009

Jamieson, A. (2015). *The hadal zone: life in the deepest oceans*. Cambridge University Press.

Lacey, N. C., Rowden, A. A., Clark, M. R., Kilgallen, N. M., Linley, T., Mayor, D. J., & Jamieson, A. J. (2016). Community structure and diversity of scavenging amphipods from bathyal to hadal depths in three South Pacific Trenches. Deep-Sea Research. Part I, Oceanographic Research Papers, 111, 121–137. https://doi.org/10.1016/j.dsr.2016.02.014

Longhurst, A. R. (1976). Interactions between zooplankton and phytoplankton profiles in the eastern tropical Pacific Ocean. *Deep-Sea Research and Oceanographic Abstracts*, *23*(8), 729–754. https://doi.org/10.1016/S0011-7471(76)80017-4

Parra, S. M., Greer, A. T., Book, J. W., Deary, A. L., Soto, I. M., Culpepper, C., Hernandez, F. J., & Miles, T. N. (2019). Acoustic detection of zooplankton diel vertical migration behaviors on the northern Gulf of Mexico shelf. Limnology and Oceanography, 64(5), 2092–2113. https://doi.org/10.1002/lno.11171

Perelman, J. N., Firing, E., van der Grient, J. M. A., Jones, B. A., & Drazen, J. C. (2021). Mesopelagic Scattering Layer Behaviors Across the Clarion-Clipperton Zone: Implications for Deep-Sea Mining. Frontiers in Marine Science, 8. https://doi.org/10.3389/fmars.2021.632764

Ryan, T. E., Downie, R. A., Kloser, R. J., & Keith, G. (2015). Reducing bias due to noise and attenuation in open-ocean echo integration data. ICES Journal of Marine Science, 72(8), 2482–2493. https://doi.org/10.1093/icesjms/fsv121

Salman, A., Siddiqui, S. A., Shafait, F., Mian, A., Shortis, M. R., Khurshid, K., Ulges, A., & Schwanecke, U. (2020). Automatic fish detection in underwater videos by a deep neural network-based hybrid motion learning system. ICES Journal of Marine Science, 77(4), 1295–1307. https://doi.org/10.1093/icesjms/fsz025

Sanford, T. B., Drever, R. G., & Dunlap, J. H. (1978). A velocity profiler based on the principles of geomagnetic induction. *Deep-Sea Research (1977)*, *25*(2), 183,IN5,197-196,IN6,210. https://doi.org/10.1016/0146-6291(78)90006-1

Sweetman, A. K., and U. Witte. "Response of an Abyssal Macrofaunal Community to a Phytodetrital Pulse." Marine Ecology. Progress Series (Halstenbek), vol. 355, 2008, pp. 73–84, https://doi.org/10.3354/meps07240.

van Haren, H., Berndt, C., & Klaucke, I. (2017). Ocean mixing in deep-sea trenches: New insights from the Challenger Deep, Mariana Trench. *Deep-Sea Research.*

Part I, Oceanographic Research Papers, *129*, 1–9. https://doi.org/10.1016/j.dsr.2017.09.003

Vinogradov, M. E. (1962). Quantitative distribution of deep-sea plankton in the western Pacific and its relation to deep-water circulation. Deep-Sea Research (1953), 8(3–4), 251–258. https://doi.org/10.1016/0146-6313(61)90026-0

Windra, A., Manik, H. M., Somantri, L., Atmadipoera, A. S., Zuraida, R., & Priatna, A. (2024). Hydroacoustic method and GIS-Dashboard visualization for fish size in Banggai Sea Waters. *BIO Web of Conferences*, *106*, 1007-. https://doi.org/10.1051/bioconf/202410601007